New Radio Sidelink with Beam Selection for Reliable Communication in High-Density Dynamic Swarms

Morejon, Santiago; Bruun, Rasmus; Fernandes, Filipa Santana da Silva; Sørensen, Troels Bundgaard; Kiilerich Pratas, Nuno; Madsen, Tatiana Kozlova; E. Mogensen, Preben

Published in:
IEEE Wireless Communications and Networking Conference, WCNC

Publication date:
2024

Document Version
Accepted author manuscript, peer reviewed version

New Radio Sidelink with Beam Selection for Reliable Communication in High-Density Dynamic Swarms

C. Santiago Morejón García*, Rasmus Liborius Bruun*, Filipa Fernandes*, Troels B. Sørensen*, Nuno K. Pratas†, Tatiana Kozlova Madsen* and Preben Mogensen*†

*Wireless Communication Networks Section, Department of Electronic Systems, Aalborg University, Denmark

†Nokia Standardization, Aalborg, Denmark

***Abstract*—Swarm production robots, an enabler for Industry 4.0, are expected to establish direct communication links with each other based on proximity. The 3GPP's New Radio sidelink is a candidate technology to enable such communication links. However, when operating in autonomous resource selection mode (mode 2), sidelink communications are prone to half-duplex and interference problems, the severity of which increases with the swarm's density. In this paper, we study how beam selection using directional antennas and context information can help reduce the impact of these problems and thus improve the reliability of packet reception. We evaluate the effect of directional antennas when applied at the transmitter and receiver, both separately and simultaneously, for increasing swarm density. Our evaluations show that these enhancements let mode 2 achieve 120% more UEs in the swarm for a 99.99% reliability target, compared to the case where these enhancements are not applied.**

***Index Terms*—NR sidelink mode 2, swarm communication, antenna directivity, reliability, beam selection, swarm production**

I. Introduction

The fourth industrial revolution currently underway (Industry 4.0) seeks, among many other aspects, to change how traditional linear and centralized production is carried out. Linear and centralized production depends on sequential manufacturing, where production modules are connected to a centralized controller. This framework makes it difficult to have the flexibility and reconfiguration capacity [1]. Swarm-based production is a suitable solution to these limitations since it will allow the production processes to be flexible and reconfigurable by separating the linear and centralized production into production modules distributed across the factory [1]. Such a framework demands stringent communication requirements among the production modules, including high reliability, high throughput, and low latency [2] [3].

In this setting, our efforts have been focused on providing robotic swarms, within an indoor factory, with high throughput data at 10 Mbps, maximum latency of 10 ms, and reliability of 99.99%, by using decentralized device-to-device (D2D) wireless communication [4]. We define reliability at the packet reception level as the percentage of packages successfully received. As a starting point, we adopted the 3^{rd} Generation Partnership Project (3GPP) framework for data transmissions. Its first specification appeared back in release 12, with proximity services (ProSe), evolving through the years to the current release 17, which focuses on Vehicle-to-everything (V2X) use cases, refered as sidelink [5], [6]. Specifically, we adopted the autonomous resource selection mode of 3GPP sidelink (SL) denoted as new radio (NR) sidelink mode 2 (mode 2) [7].

In [4] we introduced two device-centric cooperation ranges. The first one is for robots in proximity (i.e., within a radius r_c) exchanging high throughput data at 10 Mbps with a maximum latency of 10 ms and reliability of 99.99%, using mode 2 and two new proposed cooperative resource allocation schemes. In a somewhat more extensive range, $r_e > r_c$, we assume robots to periodically exchange *discovery messages* (DMs) containing context information in the form of position, heading direction, and speed. From the error-free exchange of DMs in [4], we introduced error-prone DMs in [8].

Mode 2 fulfills the stringent requirements for a swarm size of up to twenty (20) robots by using hybrid automatic repeat request (HARQ) and link adaptation by aggregation (LAAG) [9]. LAAG increases the robustness of the transmission by lowering the modulation and coding scheme (MCS) and spending more NR slots. For bigger swarms, the presence of half-duplex problems (i.e., devices selecting the same time-frequency resources for their transmission and therefore unable to hear each other's transmissions) and interference (i.e., when devices do not intend to communicate) cause the reduction of the effective signal-to-interference-plus-noise ratio (SINR), ending up in data failure receptions.

Antenna combining techniques represent a suitable solution to mitigate interference and increase the effective SINR. The selection of beams produced by directional antennas is a straightforward technique and an alternative to more complex techniques such as beamforming [10]. In [11], authors used a unmanned aerial vehicle (UAV) equipped with directional antennas to reduce the number of handovers for better reliability and lower latency. Authors in [12] used a switching system and directional antennas on a vehicle showing a considerable improvement of the reference signal received power (RSRP) and reference signal received quality (RSRQ).

In this paper, we evaluate the impact of directional antennas and beam selection in three different settings: (i) transmitter only; (ii) receiver only; and (iii) transmitter and receiver beam selection. The paper's contribution is to show how directional antennas and beam selection can significantly increase the reliability of mode 2's communication between swarm production robots 2 by using the context information transmitted in DMs [13]. We show that directional transmit and receive antennas mitigate interference in a dynamic swarm, and indirectly the effect of half-duplex problems, which would otherwise restrict mode 2 in more dense swarms. Our work differentiates from the typical beam selection procedure, which requires network assistance, [14], [15], since it is based on decentralized D2D communication and uses the context information in DMs to perform the beam selection.

In Section II, we explain and analyze mode 2's limitations (i.e., half-duplex and interference) in detail. In Section III, we present the beam selection design, which includes all the assumptions and procedures that robots follow when adopting transmitter beam selection, receiver beam selection, and the combination of both. Section IV outlines the simulation setup and results evaluation. Concluding remarks are made in Section V.

II. NR SIDELINK MODE 2 RESOURCE ALLOCATION LIMITATIONS

A UE (name adopted for the communication component incorporated in a robot) in need of data transmission must follow two procedures when using NR SL mode 2: *sensing* and *resource selection*. We assume that before these two procedures take place, UEs are time-synchronized (i.e., adopting the NR SL synchronization procedure explained in [16]). In ***sensing***, UEs scan the channel within a time window of a maximum of one-second [7], extended through the configured bandwidth, to determine the suitable candidate slots in time and frequency. The *sensing* considers the reception of the sidelink control indicator (SCI): It determines the slot's occupancy by other UE's semi-persistent (SPS) transmissions and non-SPS future transmissions. A UE considers a future slot occupied (and therefore not part of the candidate slot set) if either the *"resource reservation period"* field or the frequency and time resource assignment fields in the SCI indicate that slots during the targeted resource selection period have a signal level (*RSRP*) value above a pre-defined threshold. However, if less than 20% of all slots are candidate slots, the pre-defined *RSRP* threshold increases by 3dB. This approach continues until reaching 20%. During the ***resource selection*** procedure, the UE randomly selects the number of required slots from the set of candidate slots. When the UE establishes an SPS, these slots will be used for the UE's SPS transmission following the SPS period. To avoid persistent collisions with other UE's transmissions, the UE applies a resource re-selection counter [17] to control when it should select new resources for its SPS.

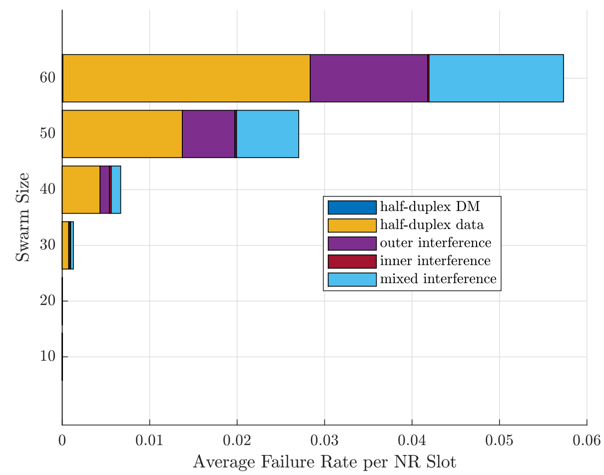

Fig. 1. Mode 2 average failure rate per NR slot and its different causes (half-duplex and interference) for different swarm sizes

A. Analysis of half-duplex problem and interference

The uncoordinated nature (i.e., the lack of coordination between the UEs) of mode 2 in the resource selection is the cause of either a half-duplex problem or interference.

1) Half-duplex problem: As introduced in Section I, UEs cannot transmit data between them if they select the same time-frequency slots. Half-duplex may impact one, several, or all data segments depending on how many slots each UE needs to transmit its data. Each data segment is transmitted in one NR slot. The more segments experiencing half-duplex problems, the higher the impact on mode 2's reliability performance.

2) Interference: Interference is caused by the harmful transmissions originating from UEs located within r_c (inner-interference) or r_e (outer-interference) of the transmitting UE. The presence of both indicates a mixed interference. These transmissions affect the SINR of the desired transmission at the receiver. In our use case it grows proportional to the swarm size as the time-frequency resource grid becomes more populated.

Fig. 1 shows mode 2's average failure rate per NR slot (the sum of per UE number of slots experiencing failures divided by the product of the swarm size and the number of slots in the simulation time) and its causes. It considers HARQ and LAAG to be enabled [9]. The antenna for these results was assumed to be isotropic, radiating the transmitted power equally in all directions. It makes sense, given the omnidirectional communication links in the specific scenario.

The absence of slots experiencing half-duplex between data and DMs (half-duplex DM) comes from the non-overlapping technique [8], which makes use of the detection of SPS transmissions during the sensing procedure to discard them as candidate slots for DM transmissions. Half-duplex data transmissions (half-duplex data) represent the predominant

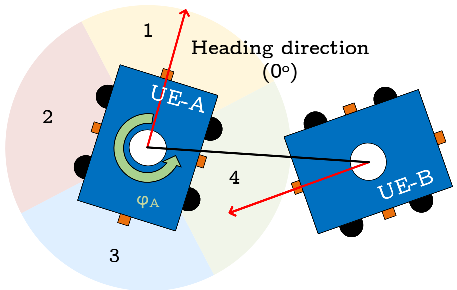

Fig. 2. Antenna selection based on the UE's orientation relative to neighbors within r_c. One patch antenna (orange square) is located on each face of the robot

cause of failures. When looking at the interference behavior, it is more likely that the interference source location is mixed (mixed interference). The reason lies in the randomness in mode 2's resource selection. If we assume that each UE uses directional antennas and beam selection, the effective SINR can be increased to mitigate the effect of the presence of half-duplex problems in one or few data segments as well as reduce the interference. As the swarm size increases, it is seen that more slots are prone to interference (in their different forms) and half-duplex data problems.

III. Beam Selection Design

A. Antenna deployment

In our design, we assume that each UE has the configuration of a type 2 vehicle [18]. Each UE has four patch antennas, each covering one of the four faces of the robot's chassis (orange squares in Fig.2). Each patch antenna produces a beam covering one of the four 90-degree horizontal azimuth sectors; hence, we interchangeably use the word beam for the same. Each sector is identified by a numbering scheme to define the robot's heading direction as sector 1 (yellow sector in Fig. 2). Sectors 2, 3, and 4 follow anti-clockwise (light red, blue, and green sectors, respectively, in Fig. 2) with reference to sector 1. The antenna numbering corresponds to the sector it covers.

B. Beam selection procedure

Our design assumes that the broadcasting/listening of DMs is done with simultaneous activation of all UE's beams. However, data transmission is reserved for the UE's transmission beam that best suits a specific target receiver UE(s). Therefore, a beam selection for transmission is required. Instead of relying on a typical power-based beam selection [19], this work proposes to leverage the context information of all neighboring robots in r_e. The context information carries each UE's coordinates, heading direction, and speed relative to a common reference frame defined for the indoor factory. It is sent by all UEs in their respective DMs and let UEs map their current and near-future locations to determine which ones will enter the critical cooperation range r_c and become target UEs for data transmission. We assume UEs can discover each other and hence receive the context information. This is a

Algorithm 1 Beam selection for UE j

Input: Context information (CI) of N UEs, $n \in S_e$, $\mid S_e \mid = N$, within r_e of UE j

for Each $k \in S_c \subseteq S_e$, $\mid S_c \mid = K \leq N$ UEs within r_c **do**

  Calculate $\phi_{j,k}$ using the latest received CI_k

  Given $\phi_{j,k}$, select the beam/sector which contains $\phi_{j,k}$

end for

Output: Beams $B_j = \{b_k\}$ for UEs $k \in S_c$, $b_k \in \{1, 2, 3, 4\}$

reasonable assumption since the DM periodicity leads to having sufficient discovery probability as stated in [8] (at least 7 DM transmissions prior to resource re-selection). It also gives UEs enough time to proceed with the beam switching. However, this does not guarantee that UEs use the most up-to-date context information, which may lead to an inaccurate estimation of the transmitter's or receiver's position. Based on the mapping, the transmitter selects the beam that exhibits the highest gain in the relative horizontal orientation (i.e., ϕ) towards the target receiver. In Fig. 2, transmitter UE–A faces UE–B at horizontal angle ϕ_A, in the direction of beam number 4, and hence only this is selected for transmission. Multiple beams can be selected if the transmitter UE has several UEs within its r_c. For example, in Fig. 2, if UE–A has an additional UE in the opposite direction of UE–B, two beams (beam number 2 and 4) are selected. An analogous beam selection process applies to data reception. Algorithm1 reflects the generic procedure UEs follow to execute the beam selection for transmitter and receiver beam selection. It is executed each time the context information is updated. If only transmitter beam selection occurs, we assume that UEs combine the output of the four patch antennas to form an isotropic receiver antenna. In this case, the transmitter can activate one or up to four beam(s) depending on the estimated locations of their desired receiver(s). More active beams will reduce the transmit power per beam (more details in Section III-D). Similarly, we assume that all UEs have an isotropic transmitter antenna but select the receiver beam that faces its transmitter for receiver beam selection only. Compared to the transmitter beam selection case, receiver beam selection is more likely to select one beam only. UEs can, however, select more than one beam in cases where they receive data from two or more transmitters. Finally, both assumptions apply if transmitter and receiver beam selection is enabled simultaneously.

C. Antenna Element Radiation Pattern

The patch antenna radiation power pattern, $A_{dB}(\theta, \phi)$, expresses how the patch spatially distributes its power through the spherical coordinates (θ, ϕ) in the vertical and horizontal planes. A generic pattern is specified by 3GPP in [20] with values of θ and ϕ between $[0^o, 180^o]$ and $[-180^o, 180^o]$, respectively:

$$A_{dB}(\theta, \phi) = 10 \times \log_{10} g(\theta, \phi), \tag{1}$$

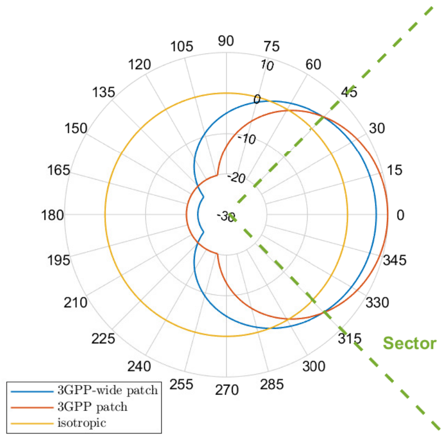

Fig. 3. Antenna pattern for 360^o azimuth angles when adopting isotropic, 3GPP modeled patch antenna element and 90-degree 3GPP modeled patch antenna element (3GPP-wide patch)

where $g(\theta, \phi)$ is the corresponding linear gain. Since the robot has four 90-degree sectors, a patch antenna covering the whole sector with the highest possible gain is the preferred option. For that purpose, we compare two values for vertical and horizontal half power beam width (HPBW), 65^o (defined in [20]) and 90^o. We name them as 3GPP patch and 3GPP-wide patch, respectively. Their normalized antenna pattern is shown in Fig. 3 together with the one of an isotropic antenna. It is noticeable that both patch antennas have the same beam gain at $\pm 45^o$, but the 3GPP patch has a higher gain within the sector. Therefore, we use the 3GPP patch model.

The vertical angle θ is fixed to 90^o since all UEs have the same height, meaning that antennas can see each other facing to the horizon, thus effectively $g(\theta, \phi) = g(\phi)$. The horizontal angle ϕ changes according to the source transmitter and/or target receiver position.

D. Signal-to-Noise-plus-Interference Ratio at the Receiver

Transmitter and receiver beam selection can work separately or simultaneously. The SINR (γ_k) in each of the K allocated slots is obtained by using the maximum ratio combining (MRC) technique with $1 \leqslant Z \leqslant 4$ received signals (on each of up to four antennas) as follows,

$$\gamma_k = \sum_{z=1}^{Z} \left(\frac{\frac{p_{tx}}{M} * \left(\sum_{j=1}^{M} \sqrt{g(\phi_{t_j})} \right)^2 * g_l * g(\phi_{r_z})}{\sum_{i=1}^{I} \left(\frac{p_{tx_i}}{M_i} * \left(\sum_{j=1}^{M_i} \sqrt{g(\phi_{t_{i_j}})} \right)^2 * g_{l_i} \right) + n} \right). \tag{2}$$

In eq. 2, $(p_{tx}, g(\phi_{t_j}), g_l)$ and $(p_{tx_i}, g(\phi_{t_{i_j}}), g_{l_i})$ are the values of transmission power, beam gain at each active transmitter beam, j, and path gain (all linear values) for the desired transmitter UE and i^{th} UE interferer(s), respectively. The beam gain at each active receiver beam is represented by $g(\phi_{r_z})$, and n is the additive white gaussian noise (AWGN).

UEs can activate M beams, from 1 to 4, with transmitter beam selection. To radiate the same transmission power regardless of the number of active beams, each time more than one beam activates, the transmission power is reduced proportionally in each of the individual beams (values M and M_i will in general differ). We assume that the transmissions from the individual beams combine coherently (voltage summation). For the case of two beams, this implies that for a UE exactly in the overlap between the beams, the effective radiated power is equal to the transmission power p_{tx}; for other "less extreme" cases, the effective transmission power is closer to half the transmission power (i.e., only one of the beams contributes significant power).

With receiver beam selection, UEs can activate Z beams from 1 to 4. It is more likely that only one beam is selected. Selecting more receive beams is generally a bad strategy since it makes the receiver more sensitive to half-duplex problems within the critical cooperation range r_c (i.e., transmissions from several transmitters within their critical cooperation range will interfere in reception).

IV. Simulation Setup and Evaluation

We implemented directional antennas and beam selection functionality to our system-level simulator in addition to the HARQ and LAAG introduced in [9]. The simulator models proximity communications for moving robots (UEs) within an indoor factory by adopting a random waypoint mobility model, providing a realistic impact of mobility and dynamics of the beam selection. The 3GPP non-line of sight indoor factory with sparse clutter and low base station (InF-SL) path loss model [20] was selected to model the path loss on the links. Furthermore, we enforced shadowing correlation using the methodology presented in [21]. We set up a de-correlation distance (δ) of 20 meters and shadow standard deviation (σ) of 5.7 dB. Proximity communication occurs when UEs have $r_c = 5$ meters (or less) distance between them. The higher layer parameter sl-PSFCH-Period-r16 is set to 1 to enable feedback in all NR slots [9]. To perform re-transmissions, one third of the transmission window (3.33 ms) is used for the first transmission, while the remaining two thirds are used for re-transmissions. Table I shows the simulation parameters settings.

When a UE needs to transmit a data message it chooses the modulation and coding scheme (MCS) for K allocated slots. The MCS is dynamically adapted to the most recently calculated γ_k. Each UE's worst γ_k is used to determine the MCS (from [7], Table 5.1.3.1-2), which can attain a block error rate (BLER) of 0.01 %. We used separate link-level simulations to generate a set of BLER curves to model the mapping from effective SINR to BLER as in [23].

To determine if the data message is successfully received or not, we calculated the effective SINR (γ_{MIC}) of K allocated resources (slots) using the mean instantaneous capacity method adopted in [9]. It is computed as,

$$\gamma_{MIC} = 2^{\frac{1}{K} \sum_{k=1}^{K} log_2(1+\gamma_k)} - 1. \tag{3}$$

TABLE I
SIMULATION PARAMETERS

Parameter	Value/range
Carrier frequency, f_c	3.5 GHz
Swarm size (number of UEs)	$[10, 20, 30, 40, 50, 60]$
Critical cooperation range, r_c	5 m
Extended Cooperation range, r_e	25 m
Facility dimensions	120×50 m^2 [20]
Transmission power, P_{tx}	0 dBm
Data channel bandwidth	100 MHz
Control channel bandwidth	7.2 MHz
NR slot duration / num. slots between Txs	250 μs / 40 NR slots
Thermal noise power spectral density	-174 dBm/Hz
Receiver noise figure	9 dB
UE speed	1 m/s
Mobility model	Random waypoint (RWP)
Pathloss model	InF-SL [20]
De-correlation distance δ	20 m [22]
Shadowing standard deviation σ	5.7 dB [22]
Discovery message periodicity	100 ms
Data message periodicity / size	10ms / 100 kb
sl-PSFCH-Period-r16	1 [9]
Scheduled Tx slots window	3.33 ms [9]
RTx slots window	6.67 ms [9]
Number of antenna elements	4
HPBW	65^o [20]
Simulation time	1000 s

In case one of the K allocated slots experiences a half-duplex problem (e.g., with DMs or other data transmissions), the spectral efficiency $(log_2(1 + \gamma_k))$ in eq. 3) is set to zero $[bps/Hz]$ on that slot. Despite a half-duplex problem represents a data loss, if the combined γ_{MIC} is sufficiently high for the selected MCS, the receiver can still decode the data message. However, if all K allocated slots experience a half-duplex problem, the receiver will not be able to decode the data message (for sure).

Our evaluations consider four configurations, namely:

1) **NR sidelink mode 2 (Baseline)** which includes mode 2's features, HARQ, LAAG, and the non-overlapping technique (introduced in [8]) to avoid half-duplex between DMs and data.
2) **NR sidelink mode 2 with transmitter beam selection (Tx)** in which, in addition to 1), transmitter beam selection is enabled.
3) **NR sidelink mode 2 with receiver beam selection (Rx)** in which, in addition to 1), receiver beam selection is enabled.
4) **NR sidelink mode 2 with transmitter and receiver beam selection (Tx&Rx)** in which both transmitter and receiver beam selection is added to 1).

We evaluate the four configurations in terms of the average failure rate per NR slot and failure probability. The latter is defined as the probability that a 100 kbit message's reception was unsuccessful within the 10 ms latency constraint. Given our previous definition of reliability, the 99.99% reliability requirement translates to a 10^{-4} failure probability.

When a UE does not experience a half-duplex problem in an allocated NR slot, the different configurations of beam selection will increment the SINR counteracting the interference (i.e., inner, outer, or mixed) effect. This increment directly impacts the value of the effective SINR, γ_{MIC}. It means that despite one or some data segments, of all allocated ones, experience half-duplex problems, data reception is more likely to occur. A benefit of this increment is that UEs require less use of HARQ and LAAG, reducing the number of NR slots used per successful data transmission.

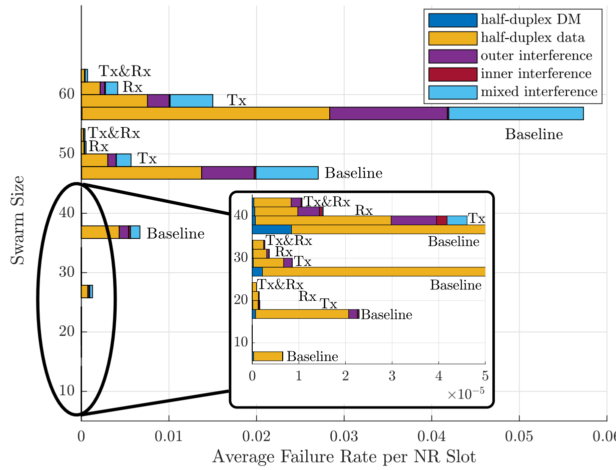

Fig. 4. Avg. failure rate per NR slot at four configurations. *Baseline* represents NR sidelink mode 2 (baseline) while *Tx beam selection*, *Rx beam selection* and *Tx&Rx beam selection* represent each of the beam selection configurations

Analyzing mode 2's average failure rate per NR slot in Fig. 4, baseline mode 2 (*Baseline* bars) experiences the highest average failure rate at all swarm sizes. The primary source of failure at small swarm sizes is half-duplex. However, interference becomes an equally contributing cause as the swarm size increases. The three beam selection configurations (*Tx, Rx, and Tx&Rx* bars) considerably reduce the average failure rate. Reducing HARQ and LAAG utilization lowers slot occupancy, causing fewer half-duplex problems. However, the number of slots experiencing interference increases as the swarm size increases. In turn, this requires more HARQ re-transmissions and the use of aggregated slots and lower MCS, hence higher resource pool occupation and average failure rate. Still, the resource pool occupancy increase does not guarantee that re-transmissions and aggregated slots will be free of failures due to the randomness of mode 2's resource selection.

Evaluating mode 2's failure probability (reliability), shown in Fig. 5, even though the baseline experiences half-duplex problems at all swarm sizes, when ten (10) UEs are in the swarm the vast majority of data segments do not experience half-duplex problems. Then, the failure probability is extremely low. As the swarm size overpasses the twenty-five (25) UEs, the baseline cannot fulfill the reliability requirement. Out of the beam selection configurations, the transmitter beam selection is the configuration with the highest proportions of half-duplex and interference problems, supporting up to thirty-eight (38)

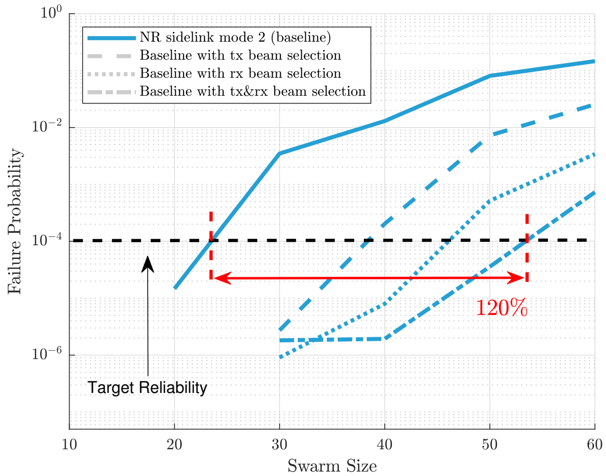

Fig. 5. Failure probability achieved at baseline and three beam selection configurations. The 10^{-4} requirement is indicated by the dashed black line.

UEs in a swarm; the transmitter is more likely to target multiple receivers, which will require the selection of more beams and increase interference. The receiver beam selection is more beneficial since receivers are more likely to receive a transmission from one transmitter at a time, using one beam, eliminating interference from the non-active beams. This allows receiver beam selection to support a swarm size of up to forty-six (46) UEs. Finally, combining both configurations allows UEs to take advantage of the focused transmission toward the receiver and simultaneously eliminate the interference on the receiver side. It supports 120% more UEs compared to the baseline.

V. Conclusions

In this paper, we evaluated three configurations using directional antennas and beam selection to reduce the failure probability of NR sidelink mode 2. The combination of transmitter and receiver beam selection allowed 120 % more UEs in the swarm compared to the baseline sidelink mode 2. At the four nines reliability, the boosting of the signal-to-noise-plus-interference ratio (SINR) at each allocated slot, together with the interference reduction, makes the effective SINR sufficiently high to decode data messages despite the presence of *half-duplex* in some NR slots. When the swarm size grows, the higher occupation of the resource pool produces more *half-duplex* problems in all slots containing data segments.

Even though transmitter and receiver beam selection together is beneficial, it requires additional means to increase the swarm size beyond fifty-three (53) UEs. Specifically, it requires a change to mode 2's resource allocation, which we have investigate in [4], [8], and [9].

References

[1] I. Rodriguez *et al.*, "5G Swarm Production: Advanced Industrial Manufacturing Concepts Enabled by Wireless Automation," *IEEE Communications Magazine*, vol. 59, no. 1, pp. 48–54, Jan. 2021.

[2] A. Varghese and D. Tandur, "Wireless requirements and challenges in industry 4.0," in *2014 International Conference on Contemporary Computing and Informatics (IC3I)*, 2014.

[3] S. K. Rao and R. Prasad, "Impact of 5G Technologies on Industry 4.0," *Wireless Personal Communications*, vol. 100, no. 1, pp. 145–159, May 2018.

[4] S. Morejón *et al.*, "Cooperative resource allocation for proximity communication in robotic swarms in an indoor factory," in *2021 IEEE Wireless Communications and Networking Conference (WCNC)*, 2021.

[5] H. Seo *et al.*, "Lte evolution for vehicle-to-everything services," *IEEE Communications Magazine*, vol. 54, no. 6, pp. 22–28, 2016.

[6] S. Chen *et al.*, "Vehicle-to-everything (v2x) services supported by lte-based systems and 5g," *IEEE Communications Standards Magazine*, vol. 1, no. 2, pp. 70–76, 2017.

[7] 3rd Generation Partnership Project (3GPP), "Physical layer procedures for data," in *3GPP TR 38.214 V16.0.0*, Dec. 2019.

[8] R. L. Bruun *et al.*, "Signaling design for cooperative resource allocation and its impact to message reliability," *IEEE Access*, vol. 11, pp. 103 569–103 584, 2023.

[9] S. Morejón *et al.*, "Decentralized cooperative resource allocation with reliability at four nines," in *2021 IEEE Global Communications Conference (GLOBECOM)*, 2021.

[10] R. Kronberger, H. Lindemier, L. Reiter, and J. Hopf, "Smart antenna application on vehicles with low profile array antennas," in *IEEE Antennas and Propagation Society International Symposium.*, vol. 2, 2000, pp. 956–959.

[11] T. Izydorczyk *et al.*, "Experimental evaluation of beamforming on uavs in cellular systems," in *2020 IEEE 92nd Vehicular Technology Conference (VTC2020-Fall)*, 2020.

[12] M. Massanet Ginard, T. Izydorczyk, P. Mogensen, and G. Berardinelli, "Enhancing vehicular link performance using directional antennas at the terminal," in *2019 IEEE Globecom Workshops (GC Wkshps)*, Dec. 2019.

[13] Y. Heng *et al.*, "Six key challenges for beam management in 5.5g and 6g systems," *IEEE Communications Magazine*, vol. 59, no. 7, pp. 74–79, 2021.

[14] L. Montero, C. Ballesteros, C. de Marco, and L. Jofre, "Beam management for vehicle-to-vehicle (v2v) communications in millimeter wave 5g," *Vehicular Communications*, vol. 34, p. 100424, 2022. [Online]. Available: https://www.sciencedirect.com/science/article/pii/S2214209621000930

[15] A. Akinsanya, M. Nair, Y. Pan, and J. Wang, "A dynamic resource allocation scheme in vehicular communications," in *IEEE INFOCOM 2020 - IEEE Conference on Computer Communications Workshops (INFOCOM WKSHPS)*, 2020, pp. 127–131.

[16] 3rd Generation Partnership Project (3GPP), "Nr radio resource control (rrc) protocol specification," in *3GPP TR 38.331 V17.1.0*, Jun. 2022.

[17] ——, "TS 38.321 V16.5.0 medium access control (mac) protocol specification," Dec. 2021.

[18] ——, "Physical channels and modulation," in *3GPP TR 37.885 V15.3.0*, Jun. 2019.

[19] M. Enescu, "Main radio interface related system procedures," in *5G New Radio a Beam-Based air Interface*. West Sussex, Sx, UK: Wiley, 2020, pp. 297-316.

[20] 3rd Generation Partnership Project (3GPP), "Study on channel model for frequencies from 0.5 to 100 ghz," in *3GPP TR 38.901 V16.1.0*, Dec. 2019.

[21] S. Lu, J. May, and R. J. Haines, "Effects of Correlated Shadowing Modeling on Performance Evaluation of Wireless Sensor Networks," in *2015 IEEE 82nd Vehicular Technology Conference (VTC2015-Fall)*. Boston, MA, USA: IEEE, Sep. 2015.

[22] ——, "Efficient modeling of correlated shadow fading in dense wireless multi-hop networks," in *2014 IEEE Wireless Communications and Networking Conference (WCNC)*. Istanbul, Turkey: IEEE, Apr. 2014.

[23] S. Lagen *et al.*, "New Radio Physical Layer Abstraction for System-Level Simulations of 5G Networks," in *ICC 2020 - 2020 IEEE International Conference on Communications (ICC)*. Dublin, Ireland: IEEE, Jun. 2020, pp. 1–7. [Online]. Available: https://ieeexplore.ieee.org/document/9149444/